Hot Spring Gas Geochemical Characteristics and Geological Implications of the Northern Yadong-Gulu Rift in the Tibetan Plateau

Xiaoli Yu[1,2]*, Zhifu Wei[1], Gen Wang[1], Xueyun Ma[1,2], Ting Zhang[1], Hui Yang[1], Liwu Li[1], Shixin Zhou[1] and Xianbin Wang[1]

[1]Key Laboratory of Petroleum Resources Research, Gansu Province, Northwest Institute of Eco-Environment and Resources, Chinese Academy of Sciences, Lanzhou, China, [2]College of Earth and Planetary Sciences, University of Chinese Academy of Sciences, Beijing, China

To reveal the heat source and its formation mechanism of the northern Yadong-Gulu rift (YGR), we analyzed the helium isotope, carbon isotope ($\delta^{13}C_{CO2}$), and CO_2/^{3}He and CH_4/^{3}He ratios of hot spring gases for tracing the source of volatiles and discussing their geological significance. The results show the following: helium is mainly derived from the crust, and the radioactive decay of the thicker crust and granites provided more ^{4}He to the low helium isotopes; thermal decomposition of carbonate rocks is the main source of CO_2; CH_4 may be of organic origin. To sum up, the gas geochemical characteristics of hot springs in the northern YGR indicate that the volatiles are mainly derived from the crust. The crust/mantle heat flow ratios (q_c/q_m) calculated by helium isotopes cover a range of 0.84–1.48, suggesting that the heat is mainly contributed by the crust. The crustal origin gas and heat flow demonstrates that the heat source beneath the northern YGR is formed by the process of interior crust. Combined with geophysical data, we suggest that the stress heat caused by the collision of the Indo-Eurasian plate and the radiant heating of the crust lead to the heat source (partial melting) and provide heat for thermal activities.

Keywords: He, CO_2, gas geochemistry, S–N trending rift, Tibetan Plateau, Yadong-Gulu rift

1 INTRODUCTION

The collision orogeny between India and Eurasia is one of the most important geological events since the Cenozoic, which led to the uplift of the Tibetan Plateau (TP). The dynamics of plateau uplifting has attracted wide attention, especially the crust–mantle structure in the collision zone (Himalayan terrane and Lhasa terrane) (Bourjot and Romanowicz, 1992; Nelson et al., 1996; Wu et al., 2005; Xu et al., 2015). The development of nearly north–south extensional rift systems in the central and southern TP is related to the dynamics of plateau uplift, and they are considered to be formed by the collapse of the orogenic plateau or regional stress changes (England and Houseman, 1989; Molnar et al., 1993; Yin and Harrison, 2000). The Yadong-Gulu rift (YGR) is the largest north–south

Abbreviations: BNS, Bangong-Nujiang suture; ITS, Indus-Tsangpo suture; JF, Jiali fault; MBT, Main Boundary Thrust.

trending rift in the central TP, which runs through the Himalayan terrane and Lhasa terrane, so it is an ideal place to study the deep structure of the collision area of the TP.

The YGR developed a large number of hot springs, and the tectonic activity is strong, which provides favorable conditions for the migration of gas from depth. Gases volatile from hot spring in the fault zone are closely related to the deep geological structure (de Moor et al., 2013; Italiano et al., 2013; Kulongoski et al., 2013). They are a mixture of gases from different sources, and their composition will significantly change due to the different physical and chemical properties of various gas components, different geological backgrounds, and different ways to enter hot springs from their sources (Wang et al., 1992). Helium is an ideal tracer in hot spring gases because it is chemically inert and its abundance is changed only by radioactive decay and physical processes during migration (Farley and Neroda, 1998). Helium has two isotopic nuclides, ^3He and ^4He. ^3He mainly derives from the mantle, while ^4He is mainly produced by the decay of uranium and thorium in the crust. The helium isotope is expressed as $^3He/^4He$, and it varies greatly with different sources (Poreda and Craig, 1989). Generally, helium includes the atmospheric source, the mantle source, and the crustal source, and their helium isotopes are 1 Ra, 8 Ra, and 0.02 Ra, respectively (Ra is atmospheric $^3He/^4He$, Ra = 1.4×10^{-6}) (Sano and Wakita, 1985). Hot spring helium isotopes have been successfully used for studying the deep geological structure in fault zones and volcanic areas (Mutlu et al., 2008; Klemperer et al., 2013). In addition, CO_2 is usually the main component of hot spring volatiles. However, the concentration and isotopes of CO_2 are easily affected by geophysical and chemical reactions in the process of migration. Therefore, $\delta^{13}C_{CO_2}$ and $CO_2/^3He$ are usually combined to explore the source of CO_2 (Zhou et al., 2020). Moreover, $CH_4/^3He$ is also used as an index to trace the source of gas (Tao et al., 2005).

Hot spring gases have also been widely applied for exploring the deep geological structure in the TP, such as in the Tengchong volcanic area in Yunnan Province (Wang et al., 1993; Xu et al., 2004; Zhao et al., 2012; Cheng et al., 2014), the Jinshajiang-Red River fault zone (Zhou et al., 2020), the Litang fault zone (Zhou et al., 2017), and the Xianshuihe-Anninghe fault zone (Xu et al., 2021). It is found that the change of hot spring gases is related to the deep heat source or the activity of fault zone. In recent years, some scholars have tried to explore the material sources (gas, fluid) and deep structures under the YGR by using hot spring gases (Zhao et al., 1998; Yokoyama et al., 1999; Zhao et al., 2002; Zhang et al., 2017), but the heat source and its formation mechanism are still under debate (Yokoyama et al., 1999; Liu et al., 2014; Zhang et al., 2017; Xie et al., 2021).

In this study, 17 hot spring gas samples were collected from the northern YGR. We analyzed the helium and carbon isotopes, $CO_2/^3He$ ratios, and $CH_4/^3He$ ratios for tracing the source of hot spring gases and discussing their geological significance to reveal the heat source and its formation mechanism of the northern YGR.
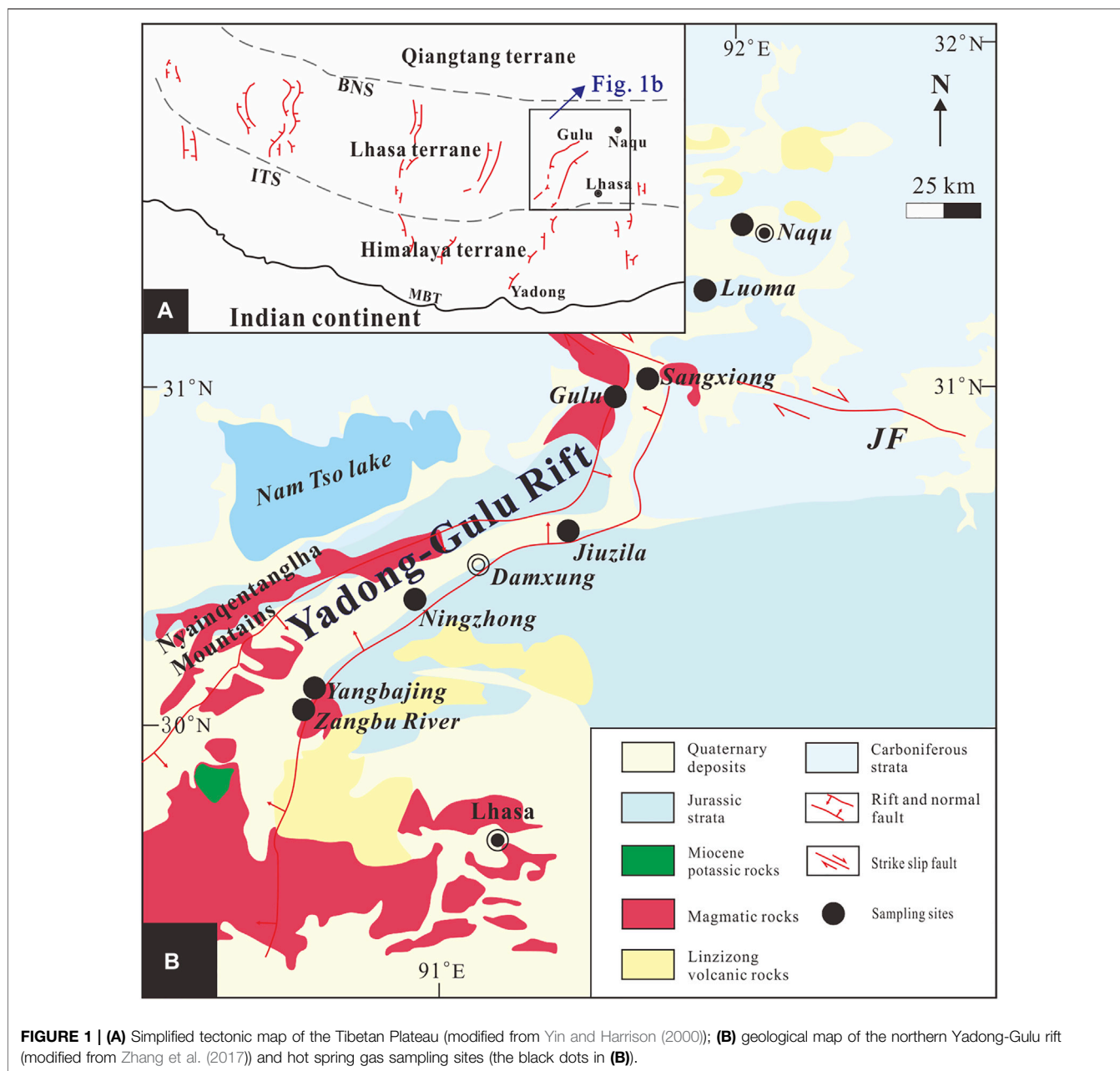
2 GEOLOGICAL SETTINGS

The Tibetan Plateau is a complex tectonic assemblage system (Yin and Harrison, 2000). It contains five relatively stable blocks,

which are the Himalayan block, Lhasa block, Qiangtang block, Songpan-Ganzi block, and Kunlun-Qilian block from south to north (Pan et al., 2012). In the southern TP, there are six junior nearly north–south trending rifts (Armijo et al., 1986; Yin, 2010), and their extensional age is from the Middle Miocene to the late Miocene (Zhang et al., 2020). The YGR is the largest rift in the TP, with a total length of nearly 600 km, which spans the Himalayan terrane and the Lhasa terrane (**Figure 1A**). The YGR can be divided into the southern, middle, and northern segments during research (Zhang et al., 2021). Our study area is mainly in the northern YGR, and it is a graben composed of two NE trending normal faults. The faults extend from Yangbajing to Sangxiong, and the northern end of the faults is cut off by a NW trending strike-slip fault (Jiali fault) (**Figure 1B**).

Due to the difference of basement and sedimentary caprocks in the Lhasa terrane, it can be divided into three subterranes with the boundaries of Shiquanhe-Nancuo melange belt (SNMB) and Luobadui-Milashan fault (LMF) (Zhu et al., 2011; Zhang et al., 2019). The northern YGR crosses the northern and central parts of the Lhasa block. The northern Lhasa has a young crust, the sedimentary caprock is a Lower Cretaceous volcanic sedimentary sequence, and the east is covered by Triassic–Jurassic strata (Zhu et al., 2013). The Middle–Upper Triassic strata are mainly composed of slate, sandstone, and radiolarian chert (Pan et al., 2006). The Precambrian basement (Zhang et al., 2012b; Dong et al., 2011), overlying Carboniferous–Permian metamorphic sedimentary rocks, and Lower Cretaceous volcanic sedimentary sequences are developed in the central Lhasa terrane, accompanied by a small amount of Ordovician, Silurian, and Triassic sedimentary rocks (Zhu et al., 2013). After collision, the Lhasa block developed multi-stage magmatism and widely developed Meso-Cenozoic igneous rocks, mainly Paleocene Gangdise granite and Linzizong volcanic rock distributed in the southern Lhasa (Wu et al., 2008).

At about 65 Ma, the Indo-Eurasian plate collided and the Indian landmass subducted beneath the Eurasian plate, resulting in the increase of crustal thickness of the southern TP (England and Houseman, 1989; Yin and Harrison, 2000; Wu et al., 2008; Pan et al., 2012), and the thickest area appeared in the Lhasa terrane, at about 80 km (Zhao et al., 1993; Zhao et al., 2001; Kind et al., 2002; Zhang et al., 2011; Li et al., 2014). The heat flow values of Yangbajing, Yangyingxiang, Laduogang, and Naqu in Lhasa are 108 m/Wm[2], 264 m/Wm[2], 338 m/Wm[2], and 319 m/Wm[2], respectively (Teng et al., 2019), which are higher than the average of Chinese mainland (63 m/Wm[2]) (Hu et al., 2000; Jiang et al., 2016; Jiang et al., 2019). Previous geophysical studies have found that many shallow low velocity and/or high conductivity zones are distributed in the crust of the Lhasa terrane, such as Yangbajing and Dangxiong, which are considered to be granitic partial melting bodies with a depth of 15–25 km and a thickness of 20 km (Brown et al., 1996; Kind et al., 1996; Nelson et al., 1996; Zhao et al., 2001).

The TP is rich in geothermal resources, and the hot springs in the Lhasa block are concentrated in the north–south trending rifts. In the northern YGR, hot springs are developed in

FIGURE 1 | (A) Simplified tectonic map of the Tibetan Plateau (modified from Yin and Harrison (2000)); **(B)** geological map of the northern Yadong-Gulu rift (modified from Zhang et al. (2017)) and hot spring gas sampling sites (the black dots in **(B)**).

Yangbajing, Ningzhong, Gulu, Naqu, and other places, with spring temperatures ranging from 23 to 87°C. The Yangbajing geothermal field is one of the non-volcanic high temperature geothermal fields in Tibet, with downhole temperatures as high as 330°C (Guo, 2012; He et al., 2012; Yuan et al., 2014; Zhang et al., 2015; Wang et al., 2022). The pH of hot spring water in the study area (such as Yangbajing, Ningzhong, and Gulu) is mostly between 7 and 9, showing a slightly alkaline property (He et al., 2012; Yuan et al., 2014; Wang et al., 2018; Guo et al., 2019). Besides, the main hydrochemical types of hot springs are mostly transitional HCO_3-Na and $Cl·HCO_3$-Na, while Yangbajing geothermal water is of Cl-Na type (Liu et al., 2014; Wang et al., 2017b).

3 SAMPLING AND ANALYSIS

Seventeen hot spring gas samples were collected from eight sites along the northern YGR (**Figure 1B**). Hot spring gas collection used the drainage gas extraction method: we used a sodium glass bottle with low helium permeability as a collection container, filled the bottle with the corresponding hot spring water, and put the bottle mouth into the hot spring water, and then the gas replaced the water. To avoid air pollution, we stopped collecting when the gas filled 2/3 of the bottle volume, and then we sealed the bottle mouth with a rubber stopper and kept the bottle mouth down during transportation and storage. In order to prevent the leakage of rare gases, gas samples were analyzed within 14 days after collection.

TABLE 1 | Chemical composition of hot spring gases in the northern Yadong-Gulu rift.

No.	Sampling site	T (°C)	H_2 (ppm)	He (ppm)	CH_4 (ppm)	O_2 (%)	CO_2 (%)	Ar (%)	N_2 (%)	N_2/Ar
1	Yangbajing 1	85	16.26	28.48	60	15.01	23.90	0.69	60.40	87.2
2	Yangbajing 2	88	20.88	93.08	270	5.56	57.46	0.58	36.10	62.1
3	Yangbajing 3	26	13.72	27.95	80	11.46	34.35	0.59	53.31	89.7
4	Yangbajing 4	85	53.49	67.21	150	11.25	37.05	0.59	50.78	86.4
5	Zangbu River 1	Nm	10.49	25.02	200	13.03	60.47	0.61	55.57	91.2
6	Zangbu River 2	Nm	15.71	45.44	150	1.03	89.74	0.19	9.02	49.6
7	Ningzhong 1	86	24.36	3.01	10	15.10	21.19	0.76	62.95	82.5
8	Ningzhong 2	77	45.90	4.86	10	13.28	34.85	0.32	51.55	163.0
9	Jiuzila	83	11.42	2.85	160	17.52	13.56	0.72	68.18	94.2
10	Gulu 1	86	402.00	49.30	490	6.07	79.03	0.27	14.53	53.2
11	Gulu 2	50	9.96	15.41	90	14.42	26.97	0.63	57.96	92.1
12	Sangxiong	Nm	6.73	292.00	140	4.23	4.30	1.03	90.40	88.1
13	Luoma 1	Nm	70.73	514.00	400	0.44	29.92	0.61	68.93	113.0
14	Luoma 2	45	11.95	48.28	240	2.20	83.04	0.28	14.45	51.6
15	Naqu 1	79	7.26	2.53	110	15.22	22.54	0.67	61.56	92.3
16	Naqu 2	10	9.06	7.17	910	9.93	43.51	0.51	45.95	89.4
17	Naqu 3	56	5.67	13.20	920	13.40	28.38	0.59	57.54	98.2

Note: Nm is the abbreviation of "not measured."

All the gas samples were tested for gas composition and isotopes in the Oil and Gas Resources Research Center of Northwest Institute of Ecological Environment and Resources, CAS. Conventional gas components were analyzed by an MAT271 Gas Mass Spectrometer with a relative standard deviation less than 0.01% and a precision of ±0.1%. The test conditions are as follows: EI ion source, ionization energy 86 eV, emission current 40 μA, ion source temperature 95°C, SIM scanning mode, and injection volume 1 ml. The abundance and isotopes of noble gases were analyzed by a VG5400 Static Vacuum Noble Gas Mass Spectrometer, and the test condition is a high voltage ion source of 9 kV and a trap current of 800 μA. Before and after analyzing the gas sample, the internal standard gas collected from the top of Gaolan Shan in Lanzhou is first tested for its noble gas components and isotopes. $\delta^{13}C_{CO2}$ was analyzed with a stable isotope ratio mass spectrometer (Thermo Fisher Scientific Delta Plus XP), and the reference value is the Pee Dee Belemnite (PDB) standard.

4 RESULTS

4.1 Chemical Compositions of Hot Spring Volatile Gases

Gas chemical compositions are listed in **Table 1**. In these hot springs, the temperature of spring water ranges from 10 to 88°C. Hot spring gases are mainly composed of N_2 and CO_2, which account for 14.53%–90.40% and 4.30%–89.74% of the total gas content, respectively. The contents of Ar and O_2 are relatively low, ranging from 0.19% to 1.03% and 0.44% to 17.52%, respectively. We found that the Ar content of Sangxiong is higher than the atmospheric value (~0.93%), indicating that there may be Ar from deep sources. The N_2/Ar ratio is a reliable index to judge whether the gas derives from the atmosphere. The atmospheric N_2/Ar is about 84, and the water-soluble gas N_2/Ar of saturated air is about 38. The N_2/Ar ratio of hot spring gas in the northern YGR is close to that of

saturated air dissolved in water and atmosphere, which is the result of infiltration of surface water into the ground and participates in the geothermal water cycle, while the N_2/Ar ratio of Ningzhong 2 is relatively higher, suggesting that there may be N_2 addition from deep structures (Kita et al., 1993). The contents of H_2, He, and CH_4 are very low, which are four orders of magnitude lower than those of the main gas components (N_2, CO_2).

4.2 Isotopic Compositions of Volatile Gases
4.2.1 Helium Isotopes
Helium isotopes are expressed as R/Ra (R is the $^3He/^4He$ value of the sample and Ra is the atmospheric $^3He/^4He$, Ra = 1.4×10^{-6}). The measured helium isotopes cover a range of 0.11–0.93 Ra (**Table 2**). In order to deduct the contamination from air, we use the $^4He/^{20}Ne$ ratio to correct R/Ra and express it as Rc/Ra, which ranges from 0.10 to 0.87 Ra. **Figure 2** shows the correlation between $^4He/^{20}Ne$ ratios. We found that the helium isotopes in Ningzhong appear near the air source, indicating that they may be affected by air contamination, while other gas samples show the characteristics of crustal origin.

4.2.2 Carbon Isotopes ($\delta^{13}C_{CO2}$)
Generally, CO_2 in hot spring gas in the geothermal area mainly includes three sources: the mantle source, the source of carbonate decomposition, and the source of decomposed organic matter in sediments. Their carbon isotopes are from −8 ‰ to 4‰, ~0‰, and less than −10‰, respectively (Dai et al., 1996; Xu et al., 2012). $\delta^{13}C_{CO2}$ of hot spring gas in the northern YGR ranges from −11.2 ‰ to 0.1‰ (versus PDB) (**Table 2**), indicating that CO_2 is mainly derived from mantle degassing and the decomposition of carbonate rock, while Gulu 1 and Sangxiong CO_2 may be organic sources.

4.3 $CO_2/^3He$ and $CH_4/^3He$ Ratios
Generally, mantle fluid has a $CO_2/^3He$ ratio of about 1.5×10^9 (Marty and Jambon, 1987), while the $CO_2/^3He$ value between 10^{12}

TABLE 2 | Isotopic compositions of He and CO_2 of hot spring gases in the northern Yadong-Gulu rift.

No.	Sampling site	$^4He/^{20}Ne$	R/Ra	Rc/Ra	q_c/q_m	$\delta^{13}C_{CO2}$ (‰)	$CO_2/^3He$ (10^8)	$CH_4/^3He$ (10^8)
1	Yangbajing 1	670.0	0.11	0.11	1.48	−5.0	530.0	1.3
2	Yangbajing 2	584.0	0.12	0.12	1.45	−6.3	380.0	1.8
3	Yangbajing 3	813.0	0.12	0.12	1.45	−5.9	730.0	1.8
4	Yangbajing 4	53.7	0.13	0.12	1.43	−4.2	330.0	1.4
5	Zangbu River 1	48.1	0.11	0.10	1.48	−5.5	800.0	5.3
6	Zangbu River 2	154.0	0.12	0.12	1.45	−6.2	1200.0	2.0
7	Ningzhong 1	0.7	0.93	0.87	0.84	−6.7	570.0	0.2
8	Ningzhong 2	0.6	0.86	0.68	0.86	−3.9	760.0	0.2
9	Jiuzila	131.0	0.44	0.44	1.06	−3.3	780.0	9.2
10	Gulu 1	114.0	0.25	0.25	1.23	−11.2	450.0	2.8
11	Gulu 2	104.0	0.25	0.25	1.23	+0.1	500.0	1.7
12	Sangxiong	32.2	0.17	0.11	1.35	−10.3	6.3	0.2
13	Luoma 1	166.0	0.23	0.23	1.26	−6.7	18.0	0.2
14	Luoma 2	80.0	0.21	0.21	1.28	−2.6	600.0	1.7
15	Naqu 1	2.4	0.57	0.50	0.98	−0.9	1250.0	5.8
16	Naqu 2	30.7	0.25	0.24	1.23	−0.7	1800.0	38.0
17	Naqu 3	200.8	0.27	0.26	1.21	−0.4	580.0	19.0

Note: $q_c/q_m = 0.815–0.300ln(^3He/^4He)$ (Wang, 2000).
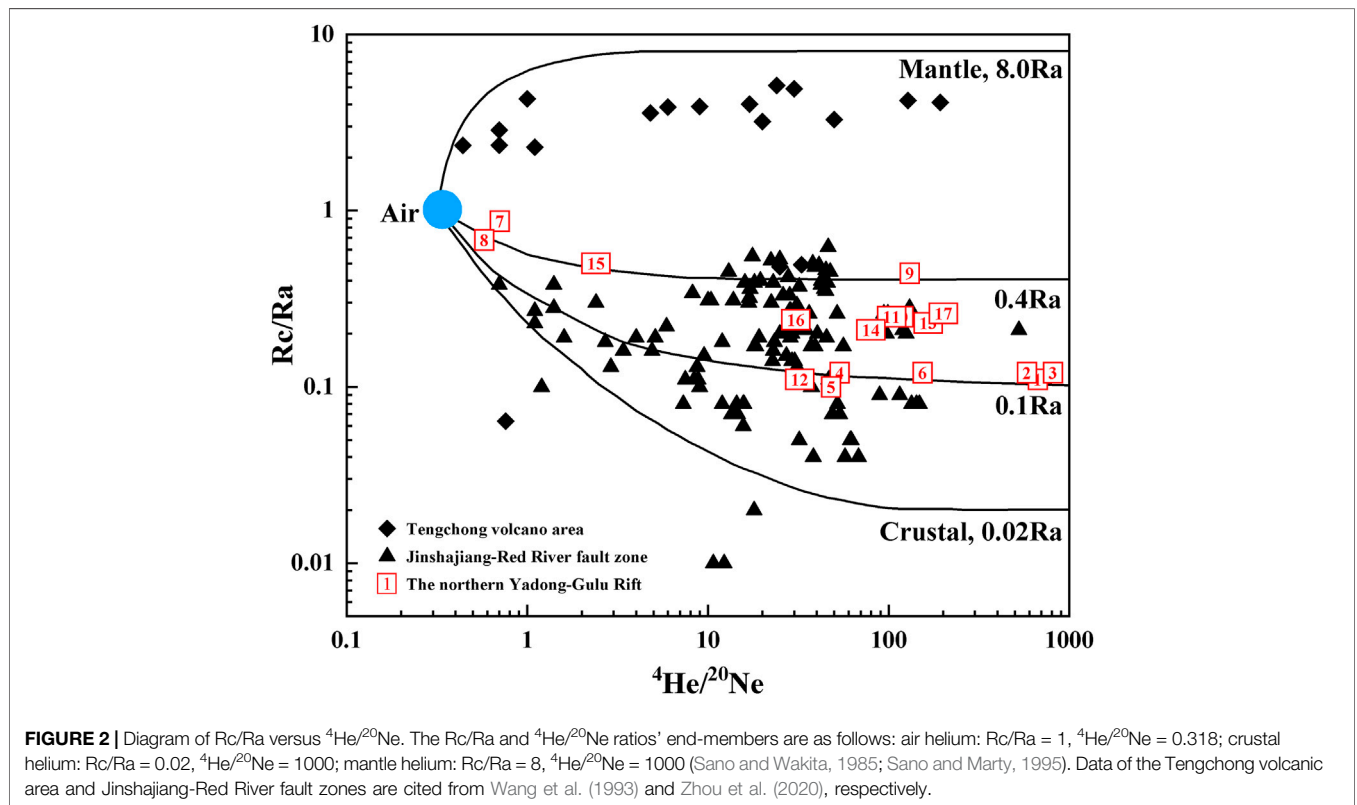
FIGURE 2 | Diagram of Rc/Ra versus $^4He/^{20}Ne$. The Rc/Ra and $^4He/^{20}Ne$ ratios' end-members are as follows: air helium: Rc/Ra = 1, $^4He/^{20}Ne$ = 0.318; crustal helium: Rc/Ra = 0.02, $^4He/^{20}Ne$ = 1000; mantle helium: Rc/Ra = 8, $^4He/^{20}Ne$ = 1000 (Sano and Wakita, 1985; Sano and Marty, 1995). Data of the Tengchong volcanic area and Jinshajiang-Red River fault zones are cited from Wang et al. (1993) and Zhou et al. (2020), respectively.

and 10^{14} is of crustal origin (limestone and sedimentary organic matter) (Sano and Marty, 1995). In our study, $CO_2/^3He$ ratios cover a range of 6.3×10^8 and 1.8×10^{11} (**Table 2**). We noted that the $CO_2/^3He$ value of Sangxiong is lower than that of the mantle, which may be affected by secondary processes (fractionation or calcite precipitation). The $CO_2/^3He$ values of Luoma 1 are close to that

of the mantle (1.5×10^9), while the higher $CO_2/^3He$ values of other hot spring gases indicate that they are derived from the crust. The $CH_4/^3He$ value can show the potential source of methane (Botz et al., 1999). The $CH_4/^3He$ ratio ranges from 0.2×10^8 to 3.8×10^9 (**Table 2**), which is larger than the value of the mantle, indicating that the gas is mainly derived from the crust (Botz et al., 1999).

5 DISCUSSION

5.1 Origin of Volatiles in the Northern YGR
5.1.1 He
Helium in the northern YGR shows obvious crustal source (Rc/Ra < 1; **Figure 2**), which may be related to the extremely thick crust and the extensive development of granites in the Lhasa terrane. At about 55 Ma, the Indian plate collided with the Lhasa terrane, and the TP began to uplift (Zhu et al., 2015). With the continuous convergence of plates, the Indian plate subducted below the lower crust of Lhasa terrane, and the crustal thickness of Lhasa terrane was twice the thickness of normal crust (Zhang et al., 2014). In the crust, abundant $^{235,\ 238}U$ and ^{232}Th will generate ^{4}He by α-radioactive decay, and the *in situ* ^{4}He concentration will gradually accumulate with the increase of time (Zhou and Ballentine, 2006). ^{4}He will be released from rocks and minerals under the tectonic activities of fault zone. As shown in **Figure 2**, the helium isotopes of hot spring gas in the YGR decrease with the increase of $^{4}He/^{20}Ne$ ratios, indicating the continuous addition of crustal helium in the process of helium transport from underground to the surface. Therefore, the thicker crustal thickness will produce more radiogenic helium, resulting in low helium isotopes, such that the helium isotopes of the Jinshajiang-Red River fault zone, which cover a range of 0.04 Ra to 0.62 Ra, show a crustal helium (**Figure 2**; Zhou et al., 2020), just like the helium characteristic in this study. A similar inference has been reported in the Karakoram fault zone on the TP (Klemperer et al., 2013). In addition, the Lhasa terrane had multi-stage magmatic intrusion (Ji et al., 2009; Zhang et al., 2014) in the process of amalgamation, convergence, and compression with the Qiangtang terrane and the Indian subcontinent. Magmatic rocks from the Mesozoic to the Miocene are developed in the YGR (Zhu et al., 2009; Zhu et al., 2011; Sun et al., 2015), mainly granites. Moreover, feldspathic granites in the late early Cretaceous are also developed outside the rift zone, such as Naqu (Sun et al., 2015). Granites contain more U and Th elements, so the radioactive decay of these two elements is one of the main sources of crustal helium in the YGR.

5.1.2 CO_2 and CH_4
In a geothermal system, the source of CO_2 may not be accurately determined just by $\delta^{13}C_{CO_2}$ because the phase separation of CO_2 between vapor and liquid will lead to the fractionation of isotopes, and it makes the gas CO_2 rich in light isotopes and has a more negative carbon isotope value (Barry et al., 2013). The $CO_2/^{3}He$ ratio is another reliable index to judge the source of CO_2. However, this index is also affected by phase separation in hydrothermal systems in the following two cases: on the one hand, the temperature is larger than $100\ ^{\circ}C$, and on the other hand, some kind of gas is supersaturated. The fractionation is mainly manifested in the difference of solubility between CO_2 and He in water, and He is more inclined to release from the liquid than CO_2. Therefore, the gas $CO_2/^{3}He$ ratio can only represent the minimum estimated value of the original value (Barry et al., 2013). Except for the hot spring gas of Sangxiong and Luoma 1, the lowest $CO_2/^{3}He$ ratio of the northern YGR is higher than that of the mantle, indicating that CO_2 is mainly derived from the crust. Combining the $CO_2/^{3}He$ ratio with $\delta^{13}C_{CO_2}$, the results show that CO_2 mainly comes from the decomposition of limestone, which is related to the lithostratigraphy of Lhasa terrane. From the middle and late early Cretaceous to the early late Cretaceous, extensive transgression occurred in Tibet. The marine strata covered most of the Lhasa terrane, and the lithofacies were composed of siliceous detritus and carbonate interbeds (Zhang et al., 2004; Zhang et al., 2012a). Therefore, CO_2 is mainly formed by thermal decarbonization of carbonate. In addition, the $CO_2/^{3}He$ ratio of Sangxiong hot spring is lower than that of the mantle, and the content of CO_2 is very low, which may be due to the loss of CO_2 in the process of gas migration. Barry et al. (2013) suggested that the precipitation of calcite will lead to the decrease of fluid $CO_2/^{3}He$ ratio. de Leeuw et al. (2010) also reported that the precipitation of calcite results in the decrease of fluid $CO_2/^{3}He$ ratio and $\delta^{13}C_{CO_2}$ at the same time. It is speculated that the $CO_2/^{3}He$ ratio in the gas will be lower. Therefore, we think that the loss of CO_2 in Sangxiong hot spring may be related to the precipitation of calcite.

$CH_4/^{3}He$ values show that CH_4 is derived from the crust. CH_4 in nature includes biogenic CH_4 and abiogenic CH_4, mainly biogenic CH_4. Biogenic methane includes two sources: microbial methane production and decomposition of sedimentary organic matter (Schoell, 1988). In addition to the abiogenic CH_4 derived from the mantle, in the strongly alkaline (pH > 10) and middle–high temperature (>150°C) hydrothermal system dominated by serpentine, abiogenic CH_4 can be synthesized by FTT reaction (Horita and Berndt, 1999; Fu et al., 2007) on the one hand, which needs to be mediated by H_2; on the other hand, it can be formed by hydration of water and olivine (Oze, 2005; Miura et al., 2011; Suda et al., 2014). However, there is no sufficient condition for the synthesis of abiotic methane because hot springs in the northern YGR have granites, sandstones, and sand conglomerates as thermal reservoirs (Liu et al., 2014), and the pH value of the hot springs is less than 10 (He et al., 2012; Yuan et al., 2014; Guo et al., 2019). Therefore, we suggested that CH_4 in the northern YGR may be of biogenic origin.

5.2 Helium in the Northern YGR and Its Geological Significance
Hot spring volatiles show great difference in geochemical characteristics in different geological background due to the difference of deep heat source. The TP is rich in geothermal resources, and its heat flows are higher than the continental mean heat flow (Jiang et al., 2016; Jiang et al., 2019), indicating a high thermal anomaly. The northern YGR and Tengchong volcanic area are all located in the Lhasa block of the TP. The heat flow value of the former is up to $319\ m/Wm^2$ (in Naqu), while that of the latter is $80–150\ m/Wm^2$ (Hu et al., 2000). With the increase of distance from the volcanic area, the heat flow value decreases gradually (Sun et al., 2016). The Tengchong volcanic area has experienced many volcanic eruptions since the late Miocene (Wang et al., 2007), and its high heat flow is considered related to lithosphere thinning caused by asthenosphere upwelling (Sun et al., 2016). The helium isotope of Tengchong hot spring is close to 8 Ra (**Figure 2**), which indicates that hot

spring gas mainly derives from mantle magmatic degassing, and this is also proved by subsequent studies on hot spring gas (Ren et al., 2005; Xu et al., 2012). However, the helium isotope of the northern YGR hot spring is less than 1 Ra, which is mainly of crustal origin. Different from the Tengchong geothermal area, the YGR is a typical non-volcanic high temperature geothermal area, and Quaternary volcanic activity has not been found (Dor, 2003). To understand the heat structure of the YGR, we calculated the crust/mantle heat flow ratio by using helium isotopes and expressed it as q_c/q_m. q_c/q_m values range from 0.84 to 1.48, indicating that the crustal heat flow is the main contributor of the heat flow (Wang, 2000; Tang et al., 2017), which is consistent with the previously reported geothermal structure of the hot crust and cold mantle in southern Tibet (Shi and Zhu, 1993). Therefore, we suggested that the heat of the northern YGR geothermal system may be contributed by the interior of the crust although other scholars suggested that there is partial melting in the boundary between the mantle and the lower crust or the upwelling of molten magma from mantle wedges beneath the northern YGR (Yokoyama et al., 1999; Zhang et al., 2017).

The heat flow values of the geotectonic unit of the TP decrease gradually from south to north, and this regional anomaly relates to deep structure (Jin et al., 2019). The INDEPTH project found seismic bright spots at the subcrustal 15–18 km in southern Tibet (from the Tsangpo suture to the Dangxiong graben), which are considered to be partial melting in the crust (Brown et al., 1996; Kind et al., 1996; Nelson et al., 1996). Therefore, the heat source of the northern YGR may be the partially melted crust (Yuan et al., 2014). However, the genetic mechanism of partial melting in the crust is still controversial. On the TP, the overlapping shear friction heat generation of the lithosphere during the collision orogeny may induce local melting in the crust, resulting in the formation of abnormal heat flux in the crust (Wang et al., 2013; Jin et al., 2019). Early geophysical and geothermal spring geochemistry studies suggested that the partial melting is silicate magma (Brown et al., 1996; Kind et al., 1996; Li and Hou, 2005). Later, Bea (2012) pointed out that radiogenic heating of the crust is usually essential for the generation of large amounts of granitic magma. 3D thermomechanical modeling simulation suggested that radioactive heat and shear heating provide the heat source for partial melting in the middle crust in Tibet (Chen et al., 2019). The latest magnetotelluric study suggested that the partial melting of the middle crust of southern Tibet was formed by crustal radiant heat and strain heating in the Miocene (Xie et al., 2021). Other geophysical studies suggested that the genesis of the YGR is related to the asthenosphere upwelling and/or the tearing of the Indian plate lithosphere (Chen et al., 2015; Wang et al., 2017a), that is, the partial melting of the crust is formed by the upwelling of mantle material. The results of helium isotope, carbon isotope, and the ratio of gas composition to ^{3}He in this study show that hot spring gas mainly derives from the crust, given the tensile age of the YGR is basically consistent with that of the melting of the middle crust, so we tend to suggest the partial melting of the YGR crust formed by the stress heat and radiation heat accumulated in the crust. Besides, the high heat flow of the Lhasa block is mainly concentrated in the north–south direction of Yangbajing–Lhasa–Naqu–Gudui area (Jiang et al., 2016), and geothermal activities are also developed in the north–south

trending rift. Nábělek and Nábělek (2014) predicted the thickness (~10–20 km) of the upper crust of brittle Tibet, which is consistent with the focal depth of the earthquake and the distribution of the crustal melting layer, indicating that the rift plays a role in connecting with the deep heat source. In addition, we have observed that high temperature hot springs are more developed in the rift than outside the rift, indicating that granite also plays an indispensable role in the supply of heat sources. Magmatic rocks are widely exposed in the rift, and the lithology is mainly granite. The radiative heat provided by granites may affect the shallow temperature of hot springs.

In a word, the helium isotopes of hot springs in the northern YGR indicate that the partial melting in the crust provides heat for the geothermal area, which was the stress heat during collision between India and Eurasia on the one hand and the radioactive heat of the crust on the other hand; the rift zone is the channel between the surface hot spring and the heat source; the local thermal difference of hot springs may be related to the distribution of granites.

6 CONCLUSION

We have analyzed the gas geochemical characteristics of hot springs in the north of Yadong-Gulu rift and found that the volatiles of hot springs are mainly derived from the crust. To further understand the geothermal structure of the Yadong-Gulu rift, we calculated the heat flow ratio of the crust to the mantle through helium isotopes and found that the heat flow is mainly contributed by the crust. Helium isotopes of hot springs indicate that the heat sources of hot springs are formed by crustal processes. Combined with the analysis of geophysical data, the results show that the tectonic heat and reflection heat of the middle crust of the Lhasa block are partially melted due to the collision of the Indo-Eurasian plate, and it provides heat for geothermal activity in the rift.

DATA AVAILABILITY STATEMENT

The original contributions presented in the study are included in the article/Supplementary Material, further inquiries can be directed to the corresponding author.

AUTHOR CONTRIBUTIONS

The idea for this article was provided by XW and XY. XY wrote the manuscript and drew the diagrams. XW, ZW, and GW guided and modified the work of this paper. HY conducted sample collection on-site. LL carried out the experimental work. TZ, XM, and SZ provided many suggestions for this article.

FUNDING

REFERENCES

Armijo, R., Tapponnier, P., Mercier, J. L., and Han, T. L. (1986). Quaternary Extension in Southern Tibet: Field Observations and Tectonic Implications. *J. Geophys. Res.* 91 (B14), 13803. doi:10.1029/JB091iB14p13803

Barry, P. H., Hilton, D. R., Fischer, T. P., de Moor, J. M., Mangasini, F., and Ramirez, C. (2013). Helium and Carbon Isotope Systematics of Cold "mazuku" CO_2 Vents and Hydrothermal Gases and Fluids from Rungwe Volcanic Province, Southern Tanzania. *Chem. Geol.* 339, 141–156. doi:10.1016/j. chemgeo.2012.07.003

Bea, F. (2012). The Sources of Energy for Crustal Melting and the Geochemistry of Heat-Producing Elements. *Lithos* 153, 278–291. doi:10.1016/j.lithos.2012. 01.017

Botz, R., Winckler, G., Bayer, R., Schmitt, M., Schmidt, M., Garbe-Schönberg, D., et al. (1999). Origin of Trace Gases in Submarine Hydrothermal Vents of the Kolbeinsey Ridge, North Iceland. *Earth Planet. Sci. Lett.* 171 (1), 83–93. doi:10. 1016/S0012-821X(99)00128-4

Bourjot, L., and Romanowicz, B. (1992). Crust and Upper Mantle Tomography in Tibet Using Surface Waves. *Geophys. Res. Lett.* 19 (9), 881–884. doi:10.1029/ 92GL00261

Brown, L. D., Zhao, W., Nelson, K. D., Hauck, M., Alsdorf, D., Ross, A., et al. (1996). Bright Spots, Structure, and Magmatism in Southern Tibet from INDEPTH Seismic Reflection Profiling. *Science* 274 (5293), 1688–1690. doi:10.1126/science.274.5293.1688

Chen, L., Song, X., Gerya, T. V., Xu, T., and Chen, Y. (2019). Crustal Melting beneath Orogenic Plateaus: Insights from 3-D Thermo-Mechanical Modeling. *Tectonophysics* 761, 1–15. doi:10.1016/j.tecto.2019.03.014

Chen, Y., Li, W., Yuan, X., Badal, J., and Teng, J. (2015). Tearing of the Indian Lithospheric Slab beneath Southern Tibet Revealed by SKS-Wave Splitting Measurements. *Earth Planet. Sci. Lett.* 413, 13–24. doi:10.1016/j.epsl.2014. 12.041

Cheng, Z. H., Guo, Z. F., Zhang, M. L., and Zhang, L. H. (2014). Carbon Dioxide Emissions from Tengchong Cenozoic Volcanic Field, Yunnan Province, SW China. *Acta Petrol. Sin.* 30 (12), 3657–3670. 1000-0569/ 2014/030(12)-3657-70.

Dai, J. X., Song, Y., Dai, C. S., Song, Y., and Wang, D. R. (1996). Geochemistry and Accumulation of Carbon Dioxide Gases in China. *Bulletin* 80 (10), 1615–1625. doi:10.1306/64EDA0D2-1724-11D7-8645000102C1865D

de Leeuw, G. A. M., Hilton, D. R., Güleç, N., and Mutlu, H. (2010). Regional and Temporal Variations in $CO_2/^3He$, $^3He/^4He$ and $\delta^{13}C$ along the North Anatolian Fault Zone, Turkey. *Appl. Geochem.* 25 (4), 524–539. doi:10.1016/ j.apgeochem.2010.01.010

de Moor, J. M., Fischer, T. P., Sharp, Z. D., Hilton, D. R., Barry, P. H., Mangasini, F., et al. (2013). Gas Chemistry and Nitrogen Isotope Compositions of Cold Mantle Gases from Rungwe Volcanic Province, Southern Tanzania. *Chem. Geol.* 339, 30–42. doi:10.1016/j.chemgeo.2012.08.004

Dong, X., Zhang, Z., Santosh, M., Wang, W., Yu, F., and Liu, F. (2011). Late Neoproterozoic Thermal Events in the Northern Lhasa Terrane, South Tibet: Zircon Chronology and Tectonic Implications. *J. Geodyn.* 52 (5), 389–405. doi:10.1016/j.jog.2011.05.002

Dor, J. (2003). The Basic Characteristics of the Yangbajing Geothermal Field —a Typical High Temperature Geothermal System. *Eng. Sci.* 5 (1), 42–47. doi:10. 3969/j.issn.1009-1742.2003.01.008

England, P., and Houseman, G. (1989). Extension during Continental Convergence, with Application to the Tibetan Plateau. *J. Geophys. Res.* 94 (B12), 17561. doi:10.1029/JB094iB12p17561

Farley, K. A., and Neroda, E. (1998). Noble Gases in the Earth's Mantle. *Annu. Rev. Earth Planet. Sci.* 26 (1), 189–218. doi:10.1146/annurev.earth.26.1.189

Fu, Q., Sherwood Lollar, B., Horita, J., Lacrampe-Couloume, G., and Seyfried, W. E. (2007). Abiotic Formation of Hydrocarbons under Hydrothermal Conditions: Constraints from Chemical and Isotope Data. *Geochimica Cosmochimica Acta* 71 (8), 1982–1998. doi:10.1016/j.gca.2007.01.022

Guo, Q. (2012). Hydrogeochemistry of High-Temperature Geothermal Systems in China: A Review. *Appl. Geochem.* 27 (10), 1887–1898. doi:10.1016/j. apgeochem.2012.07.006

Guo, Q., Planer-Friedrich, B., Liu, M., Yan, K., and Wu, G. (2019). Magmatic Fluid Input Explaining the Geochemical Anomaly of Very High Arsenic in Some Southern Tibetan Geothermal Waters. *Chem. Geol.* 513, 32–43. doi:10.1016/j. chemgeo.2019.03.008

He, L., Zhang, C. L., Dong, H., Fang, B., and Wang, G. (2012). Distribution of Glycerol Dialkyl Glycerol Tetraethers in Tibetan Hot Springs. *Geosci. Front.* 3 (3), 289–300. doi:10.1016/j.gsf.2011.11.015

Horita, J., and Berndt, M. E. (1999). Abiogenic Methane Formation and Isotopic Fractionation under Hydrothermal Conditions. *Science* 285 (5430), 1055–1057. doi:10.1126/science.285.5430.1055

Hu, S., He, L., and Wang, J. (2000). Heat Flow in the Continental Area of China: a New Data Set. *Earth Planet. Sci. Lett.* 179 (2), 407–419. doi:10.1016/S0012-821X(00)00126-6

Italiano, F., Sasmaz, A., Yuce, G., and Okan, O. O. (2013). Thermal Fluids along the East Anatolian Fault Zone (EAFZ): Geochemical Features and Relationships with the Tectonic Setting. *Chem. Geol.* 339, 103–114. doi:10.1016/j.chemgeo. 2012.07.027

Ji, W., Wu, F., Liu, C., and Chung, S. (2009). Geochronology and Petrogenesis of Granitic Rocks in Gangdese Batholith, Southern Tibet. *Sci. China Ser. D-Earth Sci.* 52 (9), 1240–1261. doi:10.1007/s11430-009-0131-y

Jiang, G., Hu, S., Shi, Y., Zhang, C., Wang, Z., and Hu, D. (2019). Terrestrial Heat Flow of Continental China: Updated Dataset and Tectonic Implications. *Tectonophysics* 753, 36–48. doi:10.1016/j.tecto.2019.01.006

Jiang, G. Z., Gao, P., Rao, S., Zhang, L. Y., Tang, X. Y., Huang, F., et al. (2016). Compilation of Heat Flow Data in the Continental Area of China. *Chin. J. Geophys.* 59 (8), 2892–2910. doi:10.6038/cjg20160815

Jin, C. S., Fu, X. G., Chen, W. B., Qiao, D. W., Ge, J., Zhu, Y. H., et al. (2019). Measurements of Borehole Heat Flow in Northern Tibet. *Chin. J. Geochem.* 62 (8), 3095–3105. doi:10.6038/cjg2019M0457

Kind, R., Ni, J., Zhao, W., Wu, J., Yuan, X., Zhao, L., et al. (1996). Evidence from Earthquake Data for a Partially Molten Crustal Layer in Southern Tibet. *Science* 274 (5293), 1692–1694. doi:10.1126/science.274.5293.1692

Kind, R., Yuan, X., Saul, J., Nelson, D., Sobolev, S. V., Mechie, J., et al. (2002). Seismic Images of Crust and Upper Mantle beneath Tibet: Evidence for Eurasian Plate Subduction. *Science* 298 (5596), 1219–1221. doi:10.1126/ science.1078115

Kita, I., Nitta, K., Nagao, K., Taguchi, S., and Koga, A. (1993). Difference in N_2/Ar Ratio of Magmatic Gases from Northeast and Southwest Japan: New Evidence for Different States of Plate Subduction. *Geol* 21 (5), 391–394. doi:10.1130/ 0091-7613(1993)021<0391:dinaro>2.3.co;2

Klemperer, S. L., Kennedy, B. M., Sastry, S. R., Makovsky, Y., Harinarayana, T., and Leech, M. L. (2013). Mantle Fluids in the Karakoram Fault: Helium Isotope Evidence. *Earth Planet. Sci. Lett.* 366, 59–70. doi:10.1016/j.epsl.2013.01.013

Kulongoski, J. T., Hilton, D. R., Barry, P. H., Esser, B. K., Hillegonds, D., and Belitz, K. (2013). Volatile Fluxes through the Big Bend Section of the San Andreas Fault, California: Helium and Carbon-Dioxide Systematics. *Chem. Geol.* 339, 92–102. doi:10.1016/j.chemgeo.2012.09.007

Li, Y., Gao, M., and Wu, Q. (2014). Crustal Thickness Map of the Chinese Mainland from Teleseismic Receiver Functions. *Tectonophysics* 611, 51–60. doi:10.1016/j.tecto.2013.11.019

Li, Z. Q., and Hou, Z. Q. (2005). "Partial Melting in the Upper Crust in Southern Tibet: Evidence from Active Geothermal Fluid System," in *Mineral Deposit Research: Meeting the Global Challenge* (Beijing, China: Springer), 1243–1245.

Liu, Z., Lin, W. J., Zhang, M., Xie, E. J., Liu, Z. M., and Wang, G. L. (2014). Geothermal Fluid Genesis and Mantle Fluids Contributions in Nimu-Naqu, Tibet. *Earth Sci. Front.* 21 (6), 356–371. doi:10.13745/j.esf.2014.06.034

Marty, B., and Jambon, A. (1987). C3He in Volatile Fluxes from the Solid Earth: Implications for Carbon Geodynamics. *Earth Planet. Sci. Lett.* 83 (1-4), 16–26. doi:10.1016/0012-821X(87)90047-1

Miura, M., Arai, S., and Mizukami, T. (2011). Raman Spectroscopy of Hydrous Inclusions in Olivine and Orthopyroxene in Ophiolitic Harzburgite: Implications for Elementary Processes in Serpentinization. *J. Mineralogical Petrological Sci.* 106 (2), 91–96. doi:10.2465/jmps.101021d

Molnar, P., England, P., and Martinod, J. (1993). Mantle Dynamics, Uplift of the Tibetan Plateau, and the Indian Monsoon. *Rev. Geophys.* 31 (4), 357–396. doi:10.1029/93RG02030

Mutlu, H., Güleç, N., and Hilton, D. R. (2008). Helium-carbon Relationships in Geothermal Fluids of Western Anatolia, Turkey. *Chem. Geol.* 247 (1-2), 305–321. doi:10.1016/j.chemgeo.2007.10.021

Nábělek, P. I., and Nábělek, J. L. (2014). Thermal Characteristics of the Main Himalaya Thrust and the Indian Lower Crust with Implications for Crustal Rheology and Partial Melting in the Himalaya Orogen. *Earth Planet. Sci. Lett.* 395, 116–123. doi:10.1016/j.epsl.2014.03.026

Nelson, K. D., Zhao, W., Brown, L. D., Kuo, J., Che, J., Liu, X., et al. (1996). Partially Molten Middle Crust beneath Southern Tibet: Synthesis of Project INDEPTH Results. *Science* 274 (5293), 1684–1688. doi:10.1126/science.274.5293.1684

Oze, C. (2005). Have Olivine, Will Gas: Serpentinization and the Abiogenic Production of Methane on Mars. *Geophys. Res. Lett.* 32 (10), L10203. doi:10.1029/2005gl022691

Pan, G. T., Mo, X. X., Hou, Z. Q., Zhu, D. C., Wang, L. Q., Li, G. M., et al. (2006). Spatial Temporal Framework of the Gangdese Orogenic Belt and its Evolution. *Acta Petrol. Sin.* 22 (3), 521–533. doi:10.3321/j.issn:1000-0569.2006.03.001

Pan, G., Wang, L., Li, R., Yuan, S., Ji, W., Yin, F., et al. (2012). Tectonic Evolution of the Qinghai-Tibet Plateau. *J. Asian Earth Sci.* 53, 3–14. doi:10.1016/j.jseaes.2011.12.018

Ren, J. G., Wang, X. B., and Ouyang, Z. Y. (2005). Mantle-derived CO2 in Hot Springs of the Rehai Geothermal Field, Tengchong, China. *Acta Geol. Sinica-English Ed.* 79 (3), 426–431. doi:10.1111/j.1755-6724.2005.tb00908.x

Poreda, R., and Craig, H. (1989). Helium Isotope Ratios in Circum-Pacific Volcanic Arcs. *Nature* 338 (6215), 473–478. doi:10.1038/338473a0

Sano, Y., and Marty, B. (1995). Origin of Carbon in Fumarolic Gas from Island Arcs. *Chem. Geol.* 119 (1-4), 265–274. doi:10.1016/0009-2541(94)00097-r

Sano, Y., and Wakita, H. (1985). Geographical Distribution of3He/4He Ratios in Japan: Implications for Arc Tectonics and Incipient Magmatism. *J. Geophys. Res.* 90 (NB10), 8729–8741. doi:10.1029/JB090iB10p08729

Schoell, M. (1988). Multiple Origins of Methane in the Earth. *Chem. Geol.* 71 (1-3), 1–10. doi:10.1016/0009-2541(88)90101-5

Shi, Y., and Zhu, Y. (1993). Some Thermotectonic Aspects of the Tibetan Plateau. *Tectonophysics* 219, 223–233. doi:10.1016/0040-1951(93)90298-X

Suda, K., Ueno, Y., Yoshizaki, M., Nakamura, H., Kurokawa, K., Nishiyama, E., et al. (2014). Origin of Methane in Serpentinite-Hosted Hydrothermal Systems: The CH4-H2-H2o Hydrogen Isotope Systematics of the Hakuba Happo Hot Spring. *Earth Planet. Sci. Lett.* 386, 112–125. doi:10.1016/j.epsl.2013.11.001

Sun, S. J., Sun, W. D., Zhang, L. P., Zhang, R. Q., Li, C. Y., Zhang, H., et al. (2015). Zircon U-Pb Ages and Geochemical Characteristics of Granitoids in Nagqu Area, Tibet. *Lithos* 231, 92–102. doi:10.1016/j.lithos.2015.06.003

Sun, Y., Wu, Z., Ye, P., Zhang, H., Li, H., and Tong, Y. (2016). Dynamics of the Tengchong Volcanic Region in the Southeastern Tibetan Plateau: A Numerical Study. *Tectonophysics* 683, 272–285. doi:10.1016/j.tecto.2016.05.028

Tang, X., Zhang, J., Pang, Z., Hu, S., Tian, J., and Bao, S. (2017). The Eastern Tibetan Plateau Geothermal Belt, Western China: Geology, Geophysics, Genesis, and Hydrothermal System. *Tectonophysics* 717, 433–448. doi:10.1016/j.tecto.2017.08.035

Tao, M., Xu, Y. C., Shi, B. G., Jiang, Z. T., Shen, P., Li, X. B., et al. (2005). Characteristics of Mantle Degassing and Deep-Seated Geological Structures in Different Typical Fault Zones of China. *Sci. China Ser. D.* 48 (7), 1074–1451. doi:10.3969/j.issn.1674-7240.2005.05.008

Teng, X. W., Song, P. H., Liu, Y. S., Zhang, X. M., Ma, X. Y., and Yan, Y. F. (2019). Deep Dynamics for the Yadong-Dongqiao-Huluhu Rift in the Tibetan Plateau. *Chin. J. Geophys.* 62 (9), 3321–3339. doi:10.6038/cjg2019L0034

Wang, C. Y., Chen, W. P., and Wang, L. P. (2013). Temperature beneath Tibet. *Earth Planet. Sci. Lett.* 375, 326–337. doi:10.1016/j.epsl.2013.05.052

Wang, G., Wei, W., Ye, G., Jin, S., Jing, J., Zhang, L., et al. (2017a). 3-D Electrical Structure across the Yadong-Gulu Rift Revealed by Magnetotelluric Data: New

Insights on the Extension of the Upper Crust and the Geometry of the Underthrusting Indian Lithospheric Slab in Southern Tibet. *Earth Planet. Sci. Lett.* 474, 172–179. doi:10.1016/j.epsl.2017.06.027

Wang, S., Liu, Z., and Shao, J. (2017b). Hydrochemistry and H-O-C-S Isotopic Geochemistry Characteristics of Geothermal Water in Nyemo-Nagqu, Tibet. *Acta Geol. Sin. - Engl. Ed.* 91 (2), 644–657. doi:10.1111/1755-6724.13123

Wang, X. B., Chen, J. F., Xu, S., Yang, H., Xue, X. F., and Wang, W. Y. (1992). Geochemical Characteristics of Hot Spring Gas in Seismic Area. *Sci. China* 8, 849–854.

Wang, X. B., Xu, S., Chen, J. F., Sun, M. L., Xue, X. F., and Wang, W. Y. (1993). Gas Chemical and Helium Isotopic Composition of Hot Springs in Tengchong Volcano Area. *Chin. Sci. Bull.* 38 (9), 814–817. CNKI:SUN:KXTB.0.1993-09-014.

Wang, X., Wang, G., Lu, C., Gan, H., and Liu, Z. (2018). Evolution of Deep Parent Fluids of Geothermal Fields in the Nimu-Nagchu Geothermal Belt, Tibet, China. *Geothermics* 71, 118–131. doi:10.1016/j.geothermics.2017.07.010

Wang, Y., Li, L., Wen, H., and Hao, Y. (2022). Geochemical Evidence for the Nonexistence of Supercritical Geothermal Fluids at the Yangbajing Geothermal Field, Southern Tibet. *J. Hydrology* 604, 127243. doi:10.1016/j.jhydrol.2021.127243

Wang, Y. (2000). Using Helium Isotope Composition in Underground Fluid to Estimate the Ratio of Crust/mantle Component of Continental Heat Flow. *Chin. J. Geophys.* 43 (6), 805–815. doi:10.1002/cjg2.97

Wang, Y., Zhang, X., Jiang, C., Wei, H., and Wan, J. (2007). Tectonic Controls on the Late Miocene-Holocene Volcanic Eruptions of the Tengchong Volcanic Field along the Southeastern Margin of the Tibetan Plateau. *J. Asian Earth Sci.* 30 (2), 375–389. doi:10.1016/j.jseaes.2006.11.005

Wu, F. Y., Huang, B. C., Ye, K., and Fang, A. M. (2008). Collapsed Himalayan - Tibetan Orogen and the Rising Tibetan Plateau. *Acta Geosci. Sin.* 24 (1), 30. doi:10.3986/AGS48106

Wu, Q., Zeng, R., and Zhao, W. (2005). The Upper Mantle Structure of the Tibetan Plateau and its Implication for the Continent-Continent Collision. *Sci. China Ser. D-Earth Sci.* 48 (8), 1158–1164. doi:10.1360/03yd0556

Xie, C., Jin, S., Wei, W., Ye, G., Jing, J., Zhang, L., et al. (2021). Middle Crustal Partial Melting Triggered since the Mid-Miocene in Southern Tibet: Insights from Magnetotelluric Data. *J. Geophys Res. Solid Earth* 126 (9), e2021JB022435. doi:10.1029/2021jb022435

Xu, Q., Zhao, J., Yuan, X., Liu, H., and Pei, S. (2015). Mapping Crustal Structure beneath Southern Tibet: Seismic Evidence for Continental Crustal Underthrusting. *Gondwana Res.* 27 (4), 1487–1493. doi:10.1016/j.gr.2014.01.006

Xu, S., Zheng, G. D., and Xu, Y. C. (2012). Helium, Argon and Carbon Isotopic Compositions of Spring Gases in the Hainan Island, China. *Acta Geosci. Sin. Engl. Ed.* 86 (6), 1515–1523. doi:10.1111/1755-6724.12019

Xu, S., Nakai, S. i., Wakita, H., and Wang, X. B. (2004). Carbon and Noble Gas Isotopes in the Tengchong Volcanic Geothermal Area, Yunnan, Southwestern China. *Acta Geol. Sinica-English Ed.* 78 (5), 1122–1135. doi:10.1111/j.1755-6724.2004.tb00769.x

Xu, S., Guan, L., Zhang, M., Zhong, J., Liu, W., Xie, X. g., et al. (2021). Degassing of Deep-Sourced CO2 from Xianshuihe-Aninghe Fault Zones in the Eastern Tibetan Plateau. *Sci. China Earth Sci.* 65 (1), 139–155. doi:10.1007/s11430-021-9810-x

Yin, A. (2010). Cenozoic Tectonic Evolution of Asia: A Preliminary Synthesis. *Tectonophysics* 488 (1-4), 293–325. doi:10.1016/j.tecto.2009.06.002

Yin, A., and Harrison, T. M. (2000). Geologic Evolution of the Himalayan-Tibetan Orogen. *Annu. Rev. Earth Planet. Sci.* 28 (1), 211–280. doi:10.1146/annurev.earth.28.1.211

Yokoyama, T., Nakai, S. I., and Wakita, H. (1999). Helium and Carbon Isotopic Compositions of Hot Spring Gases in the Tibetan Plateau. *J. Volcanol. Geotherm. Res.* 88 (1), 99–107. doi:10.1016/S0377-0273(98)00108-5

Yuan, J., Guo, Q., and Wang, Y. (2014). Geochemical Behaviors of Boron and its Isotopes in Aqueous Environment of the Yangbajing and Yangyi Geothermal Fields, Tibet, China. *J. Geochem. Explor.* 140, 11–22. doi:10.1016/j.gexplo.2014.01.006

Zhang, J. W., Li, H. A., Zhang, H. P., and Xu, X. Y. (2020). Research Progress in Cenozoic N-S Striking Rifts in Tibetan Plateau. *Adv. Earth Sci.* 35 (8), 848–862. doi:10.11867/j.issn.1001-8166.2020.064

Zhang, K. J., Xia, B. D., Wang, G. M., Li, Y. T., and Ye, H. F. (2004). Early Cretaceous Stratigraphy, Depositional Environments, Sandstone Provenance, and Tectonic Setting of Central Tibet, Western China. *Geol. Soc. Am. Bull.* 116 (9), 1202. doi:10.1130/b25388.1

Zhang, K. J., Zhang, Y. X., Tang, X. C., and Xia, B. (2012a). Late Mesozoic Tectonic Evolution and Growth of the Tibetan Plateau Prior to the Indo-Asian Collision. *Earth-Science Rev.* 114 (3-4), 236–249. doi:10.1016/j.earscirev.2012.06.001

Zhang, L. X., Wang, Q., Zhu, D. C., Li, S. M., Zhao, Z. D., Zhang, L. L., et al. (2019). Generation of Leucogranites via Fractional Crystallization: A Case from the Late Triassic Luoza Batholith in the Lhasa Terrane, Southern Tibet. *Gondwana Res.* 66, 63–76. doi:10.1016/j.gr.2018.08.008

Zhang, L., Guo, Z., Sano, Y., Zhang, M., Sun, Y., Cheng, Z., et al. (2017). Flux and Genesis of CO_2 Degassing from Volcanic-Geothermal Fields of Gulu-Yadong Rift in the Lhasa Terrane, South Tibet: Constraints on Characteristics of Deep Carbon Cycle in the India-Asia Continent Subduction Zone. *J. Asian Earth Sci.* 149, 110–123. doi:10.1016/j.jseaes.2017.05.036

Zhang, M., Guo, Z., Xu, S., Barry, P. H., Sano, Y., Zhang, L., et al. (2021). Linking Deeply-Sourced Volatile Emissions to Plateau Growth Dynamics in Southeastern Tibetan Plateau. *Nat. Commun.* 12 (1), 4157. doi:10.1038/s41467-021-24415-y

Zhang, W., Tan, H., Zhang, Y., Wei, H., and Dong, T. (2015). Boron Geochemistry from Some Typical Tibetan Hydrothermal Systems: Origin and Isotopic Fractionation. *Appl. Geochem.* 63, 436–445. doi:10.1016/j.apgeochem.2015.10.006

Zhang, Z., Deng, Y., Teng, J., Wang, C., Gao, R., Chen, Y., et al. (2011). An Overview of the Crustal Structure of the Tibetan Plateau after 35 Years of Deep Seismic Soundings. *J. Asian Earth Sci.* 40 (4), 977–989. doi:10.1016/j.jseaes.2010.03.010

Zhang, Z., Dong, X., Liu, F., Lin, Y., Yan, R., He, Z., et al. (2012b). The Making of Gondwana: Discovery of 650Ma HP Granulites from the North Lhasa, Tibet. *Precambrian Res.* 212-213, 107–116. doi:10.1016/j.precamres.2012.04.018

Zhang, Z. M., Dong, X., Santosh, M., and Zhao, G. C. (2014). Metamorphism and Tectonic Evolution of the Lhasa Terrane, Central Tibet. *Gondwana Res.* 25 (1), 170–189. doi:10.1016/j.gr.2012.08.024

Zhao, C. P., Ran, H., and Wang, Y. (2012). Present-day Mantle-Derived Helium Release in the Tengchong Volcanic Field, Southwest China: Implications for Tectonics and Magmatism. *Acta Petrol. Sin.* 28 (4), 1189–1204. 1000-0569/2012/028 (04) -1189-04. doi:10.3724/sp.j.1260.2012.20042

Zhao, P., Dor, J., Liang, T., Jin, J., and Zhang, H. (1998). Characteristics of Gas Geochemistry in Yangbajing Geothermal Field, Tibet. *Chin. Sci. Bull.* 43 (7), 1770–1777. doi:10.1007/BF02883369

Zhao, P., Xie, E. J., Dor, J., Jin, J., Hu, X. C., Du, S. P., et al. (2002). Chemical Characteristics of Geothermal Gases and Their Geological Implications in Tibet. *Acta Petrol. Sin.* 18 (4), 539–550. doi:10.1002/poc.1772

Zhao, W., Mechie, J., Brown, L. D., Guo, J., Haines, S., Hearn, T., et al. (2001). Crustal Structure of Central Tibet as Derived from Project INDEPTH Wide-Angle Seismic Data. *Geophys. J. Int.* 145 (2), 486–498. doi:10.1046/j.0956-540x.2001.01402.x

Zhao, W., Nelson, K. D., Che, J., Quo, J., Lu, D., Wu, C., et al. (1993). Deep Seismic Reflection Evidence for Continental Underthrusting beneath Southern Tibet. *Nature* 366 (6455), 557–559. doi:10.1038/366557a0

Zhou, X. C., Wang, W. L., Li, L. W., Hou, J. M., Xing, L. T., Li, Z. P., et al. (2020). Geochemical Features of Hot Spring Gases in the Jinshajiang-Red River Fault Zone, Southeast Tibetan Plateau. *Acta Petrol. Sin.* 36 (7), 2197–2214. doi:10.18654/1000-0569/2020.07.18

Zhou, X., Liu, L., Chen, Z., Cui, Y., and Du, J. (2017). Gas Geochemistry of the Hot Spring in the Litang Fault Zone, Southeast Tibetan Plateau. *Appl. Geochem.* 79, 17–26. doi:10.1016/j.apgeochem.2017.01.022

Zhou, Z., and Ballentine, C. J. (2006). 4He Dating of Groundwater Associated with Hydrocarbon Reservoirs. *Chem. Geol.* 226 (3-4), 309–327. doi:10.1016/j.chemgeo.2005.09.030

Zhu, D. C., Mo, X. X., Niu, Y., Zhao, Z. D., Wang, L. Q., Liu, Y. S., et al. (2009). Geochemical Investigation of Early Cretaceous Igneous Rocks along an East-West Traverse throughout the Central Lhasa Terrane, Tibet. *Chem. Geol.* 268 (3-4), 298–312. doi:10.1016/j.chemgeo.2009.09.008

Zhu, D. C., Wang, Q., Zhao, Z. D., Chung, S. L., Cawood, P. A., Niu, Y., et al. (2015). Magmatic Record of India-Asia Collision. *Sci. Rep.* 5, 14289. doi:10.1038/srep14289

Zhu, D. C., Zhao, Z. D., Niu, Y., Dilek, Y., Hou, Z. Q., and Mo, X. X. (2013). The Origin and Pre-cenozoic Evolution of the Tibetan Plateau. *Gondwana Res.* 23 (4), 1429–1454. doi:10.1016/j.gr.2012.02.002

Zhu, D.-C., Zhao, Z. D., Niu, Y., Mo, X. X., Chung, S. L., Hou, Z. Q., et al. (2011). The Lhasa Terrane: Record of a Microcontinent and its Histories of Drift and Growth. *Earth Planet. Sci. Lett.* 301 (1-2), 241–255. doi:10.1016/j.epsl.2010.11.005

Conflict of Interest: The authors declare that the research was conducted in the absence of any commercial or financial relationships that could be construed as a potential conflict of interest.

Publisher's Note: All claims expressed in this article are solely those of the authors and do not necessarily represent those of their affiliated organizations, or those of the publisher, the editors and the reviewers. Any product that may be evaluated in this article, or claim that may be made by its manufacturer, is not guaranteed or endorsed by the publisher.